Full Assignment of the ^{13}C NMR Spectra of Regioregular Polypropylenes: Methyl and Methylene Region

Vincenzo Busico,* Roberta Cipullo, Guglielmo Monaco, and Michele Vacatello

Dipartimento di Chimica, Università di Napoli "Federico II", Via Mezzocannone, 4, 80134 Napoli, Italy

Anna Laura Segre

Istituto di Strutturistica Chimica and NMR Service—CNR Research Area, C.P. 10, Monterotondo Stazione, 00016 Roma, Italy

Received April 4, 1997; Revised Manuscript Received June 18, 1997[⊗]

ABSTRACT: ^{13}C NMR spectroscopy is the main source of information on the stereochemistry of Ziegler−Natta and related transition metal catalyzed propene polymerizations. In simple cases, like those of polypropylenes formed under pure enantiomorphic-site or chain-end control, the origin of the stereoselectivity can be easily recognized from the steric pentad distribution obtained from routine ^{13}C NMR spectra. On the other hand, the variety of innovative polymers that can now be prepared with "high-yield" heterogeneous and metallocene-based homogeneous catalysts under hybrid, multiple, or oscillating stereocontrol represent very complex systems, which are beyond the possibilities of configurational analysis by routine ^{13}C NMR. In such cases, high-field ^{13}C NMR can be highly advantageous. Indeed, in this paper we show that from the methyl and methylene regions of 150 MHz ^{13}C NMR spectra of polypropylenes of various tacticities, the stereosequence distribution can be determined at a much finer level of detail, so as to obtain an adequate experimental basis for the investigation of the many complicated mechanisms of stereocontrol presently encountered in Ziegler−Natta catalysis.

Introduction

A polymer chain is—in a way—a permanent record of the statistical chain of events which constituted the polymerization process. From its microstructure, it is possible to identify the various monomer reaction modes, to measure their relative rates, and even—at least in principle—to infer their interdependence: the longer the chain segment that can be examined, the richer is its message.

In this respect, ^{13}C NMR has proved to be a fundamental technique, particularly in the field of Ziegler−Natta and related transition metal catalyzed 1-alkene polymerizations.[1−4]

Many of these processes are highly stereoselective, and the distribution of configurations in the polymers is obviously related to the mechanism of stereocontrol.[1−3,5,6] Importantly, the chemical shift of a ^{13}C nucleus in a poly(1-alkene) chain is a function not only of the constitution of the chain segment in which it is located but also of its average conformation, which in turn depends on the configuration;[2,7] this is the basis for ^{13}C NMR stereosequence analysis, the most powerful tool for tracing the origin of the stereoselectivity of active species which are normally unaccessible to direct observations.[1,3,7]

By coincidence, the resolution of ^{13}C NMR is maximum for the poly(1-alkene) of highest industrial significance—namely polypropylene. In a typical "routine" spectrum[8] recorded at 50−75 MHz, the methyl resonance, in particular, is split into components corresponding to the steric pentads.[1−3,7] In simple cases, such as those of polymers formed under pure enantiomorphic-site[5] or chain-end[6] control, the configurational statistics can be recognized at a glance.[1−3]

Only when the stereoregularity is very low does the identification become more difficult. Due to the increased number of broad and partly overlapped peaks, a quantitative evaluation of the spectrum may be required. The common practice is to perform a best-fit of the normalized experimental integrals with theoretical ones calculated in terms of tentative statistical models, by solving in the least-squares sense the overdetermined set of (usually cumbersome) equations which give the probability of occurrence of each observable pentad.[3]

On the other hand, the variety of unique polypropylenes that can be obtained with "high-yield" heterogeneous[9] and metallocene-based homogeneous[1c] catalysts under hybrid,[10] multiple, or oscillating[3d,11] stereocontrol represent much more complex cases. Their configurational study requires the use of statistical models with several adjustable parameters, which are beyond the possibility of quantitative analysis at the pentad level.

In these cases, high-field ^{13}C NMR can be highly advantageous. As a matter of fact, we have already shown[3d,f] that, in the 150 MHz ^{13}C NMR spectra of polypropylenes of various tacticities, methyl resonances associated with different steric pentads are well separated and reveal their fine structure at heptad/nonad levels even for samples of low stereoregularity.

In ref 3f, we reported a first set of assignments opening the way to more rigorous statistical calculations. To this end, in the same paper we also introduced computational methods in which the traditional analytical treatment is replaced by conceptually simpler matrix multiplication techniques; it is important to note that these methods, apart from being more practical for handling data on stereosequences longer than pentads, allow one to take into account the hypothesis of reversible switches between different types of stereocontrol.

We have now completed our study, ending up with a full assignment of the 150 MHz ^{13}C NMR spectra of regioregular polypropylenes.

In this paper, we report the assignments of the methyl and methylene resonances; those of the methine reso-

[⊗] Abstract published in *Advance ACS Abstracts,* August 15, 1997.

S0024-9297(97)00466-X CCC: $14.00

Chart 1

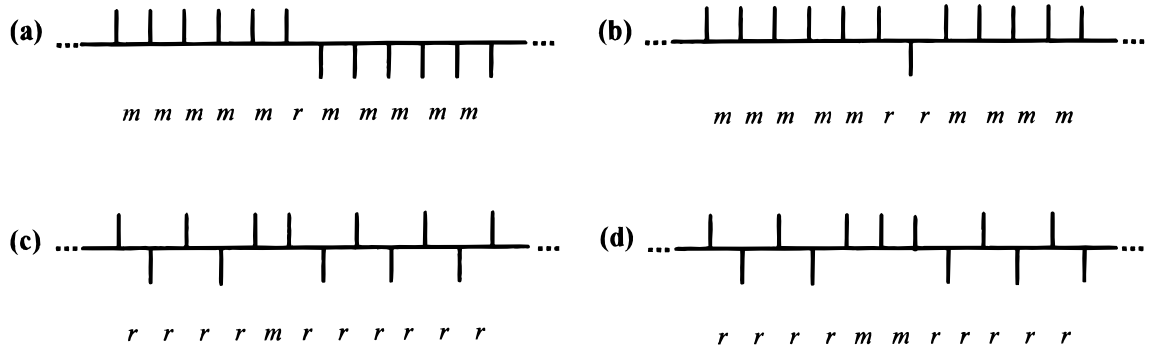

Chart 2

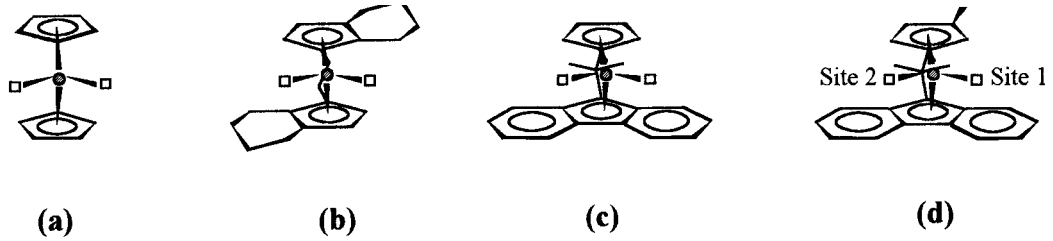

nances, which required an adaptation of the standard semiempirical methods for chemical shift predictions in terms of the "*γ-gauche* effect",[7c] will be discussed in a separate paper.

An adequate and reliable basis has thus been obtained for the investigation of the complicated mechanisms of stereocontrol presently encountered in Ziegler−Natta and metallocene-catalyzed stereoselective propene polymerizations, as will be shown in forthcoming papers.

Results and Discussion

Description of the Model Polypropylene Samples. For our study, we selected four model polypropylene samples obtained in the presence of suitable "single-site" metallocene catalysts,[1c] with distributions of configurations corresponding to four different statistical models and able to give rise to the widest possible set of stereosequences.

A predominantly isotactic polypropylene with stereodefects of the ...*mmmrmmm*... type (Chart 1a), resulting from a chain-end mechanism of stereocontrol[6] (*1,3-lk* asymmetric induction), was obtained in the presence of the catalyst system bis(cyclopentadienyl)$TiCl_2$ (Chart 2a)/MAO (MAO = methylalumoxane) at low temperature[12] (sample A, fraction of *meso* diads, $[m] \approx 0.80$).

A second predominantly isotactic polypropylene with randomly distributed stereoerrors of the ...*mmmrrmmm*... type (Chart 1b) was prepared with the catalyst system *rac*-ethylenebis(4,5,6,7-tetrahydro-1-indenyl)-$ZrCl_2$[13] (Chart 2b)/MAO (sample B, $[m] \approx 0.70$). The stereosequence distribution of this sample can be described in terms of the enantiomorphic-site statistics,[5] in spite of the fact that most stereoirregularities are not due to monomer insertions with the less reactive enantioface but to a side reaction of epimerization of the growing polymer chain.[14]

A predominantly syndiotactic polypropylene was obtained in the presence of Me_2C(cyclopentadienyl)(9-fluorenyl)$ZrCl_2$[15,16] (Me = methyl; Chart 2c)/MAO (sample C, fraction of *racemic* diads, $[r] \approx 0.80$). The syndiotactic selectivity of this C_s-symmetric metallocene catalyst is the result of a "chain migratory" propagation mechanism, with the incoming monomer and the growing polymer chain exchanging regularly at each insertion step between the two enantiotopic coordination positions available at the transition metal atom.[16] Failures of this mechanism ("skipped insertions") lead to the formation of ...*rrrrmrrrr*... stereodefects (Chart 1c), which sum up to ...*rrrrmmrrrr*... ones (Chart 1d) arising from occasional monomer misinsertions.[16]

The polymerization conditions (see Experimental Section) were adjusted so as to produce samples with a degree of stereoregularity low enough to result in appreciable fractions of short stereosequences (hexads to undecads) containing up to three stereoerrors, but not to the point that the predominant tacticity could not be recognized on inspection from their ^{13}C NMR spectra.

A fourth model polypropylene with hemiisotactic structure,[17] prepared with the catalyst system Me_2C-(3-Me-cyclopentadienyl)(9-fluorenyl)$ZrCl_2$[18] (Chart 2d)/MAO (sample D), was received from Professor G. Di Silvestro.

The methyl and methylene regions of the 150 MHz ^{13}C NMR spectra of samples A−D, recorded at 70 °C on dilute solutions in 1,1,2,2-tetrachloroethane-d_2, are shown in Figures 1 and 2, respectively. The chemical shift values of about 100 observed resonances are listed in Tables 1−4 (one table for each model polymer, for easier consultation); their reproducibility was found to be ±1 Hz, roughly corresponding to ±0.002 ppm. For each of the two spectral regions, the peaks were numbered progressively from low field to high field, taking into account all four spectra. Due to the different tacticities of the polymers examined, it is hard to select a specific stereosequence as a logical common origin of the relative chemical shift scale; therefore, we chose to refer all resonances to the solvent, by setting the central line of the triplet of 1,1,2,2-tetrachloroethane-d_2 at $\delta =$ 74.3 ppm downfield of tetramethylsilane (TMS).

Predictive Methods for the Configurational Dependence of Polypropylene Chemical Shifts: Scope and Limitations. Semiempirical methods for predicting the effect of the configuration on the chemical shifts of regioregular polypropylenes have been proposed in a number of publications.[2c−l,7c] These methods require the combination of (at least) two models: one for describing

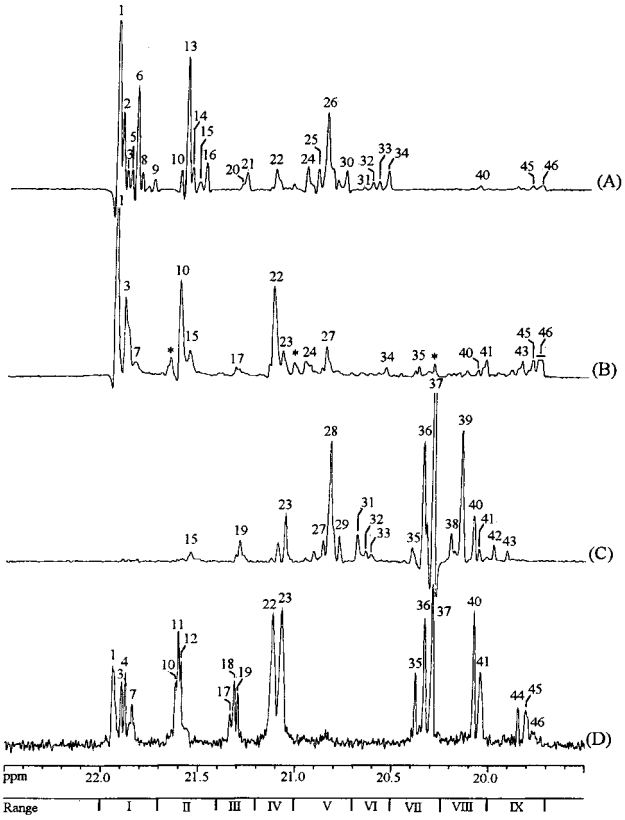

Figure 1. Methyl region of the 150 MHz ^{13}C NMR spectra of the four model polypropylene samples A−D (dissolved in 1,1,2,2-tetrachloroethane-d_2 at 70 °C); δ scale is in ppm downfield of TMS. For peak assignments, see Tables 1−4. In the spectrum of sample B, resonances arising from chain end groups and/or regioirregular sequences are marked with asterisks (*).

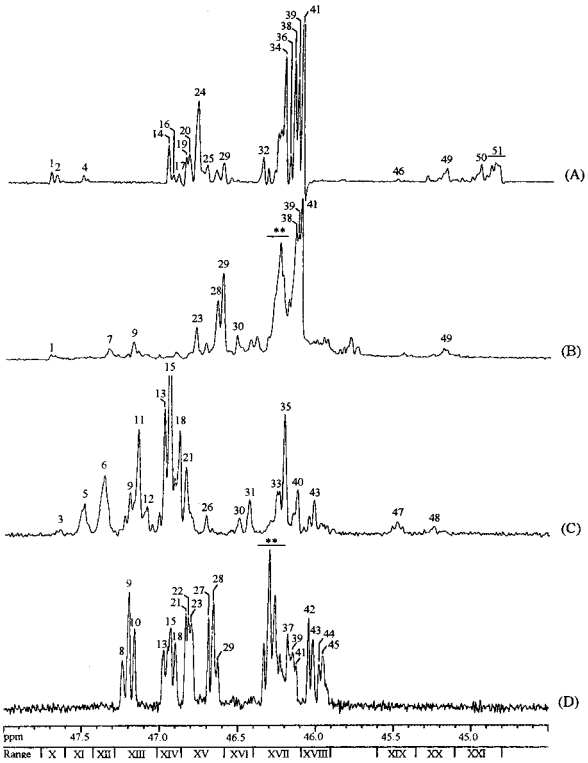

Figure 2. Methylene region of the 150 MHz ^{13}C NMR spectra of the four model polypropylene samples A−D (dissolved in 1,1,2,2-tetrachloroethane-d_2 at 70 °C); δ scale is in ppm downfield of TMS. For peak assignments, see Tables 1−4. In the spectra of samples B and D, the broad multiplet marked with a double asterisk (**), which receives contributions from the *rmmmr*, *rrrrm*, *mmrrm*, and/or *rmrrr* hexads, is too complex for attempting a detailed assignment.

the conformational statistics (which depends on the configuration); another for weighting the conformers with appropriate contributions to the chemical shift (*i.e.*, with conformational screen parameters).

What is normally done is to adopt the rotational isomeric state (RIS) approximation[19] and to ascribe the effect of the conformation on the chemical shift δ of a magnetic carbon $\bar{C}$ to changes in populations of rotamers differing only for the $\bar{C}$ $-C(\alpha)-C(\beta)-C(\gamma)$ dihedral angle. This can be translated in the following formula:

$$\delta = \delta_0 + \sum_i \gamma_i p_i \qquad (1)$$

where δ_0 is the conformation-independent part of δ, p_i is the sum of the probabilities that each of the C(α)−C(β) bonds flanking $\bar{C}$ be in the ith rotational isomeric state, and γ_i is the contribution to δ of such state.

A further common approximation is to assume that in eq 1 $\gamma_i \neq 0$ only when $\bar{C}$ and C(γ) are in a *gauche* arrangement ("*γ-gauche* effect").[7c]

In a first quantitative study,[2c] Provasoli and Ferro made use of the RIS model of Boyd and Breitling[20] and of an existing set of methyl resonance attributions at pentad level[2b] to estimate the magnitude of the γ parameter in terms of the *γ-gauche* effect. Later on, Ferro *et al.* published the results of improved calculations for the methyl and methylene C's using eq 1 in its general form.[2e,f]

The more advanced RIS model of Suter and Flory[21] was adopted instead by Tonelli,[2d] who reported (in collaboration with Schilling) calculations for the ^{13}C methyl, methylene, and methine resonances at heptad, hexad, and pentad level, respectively.[2g]

More recent analyses of ^{13}C NMR spectra of polypropylene (recorded in all cases with spectrometers operating below 100 MHz) in terms of *γ-gauche* predictions can be found in refs 2h−l and 7c. For short stereosequences (pentads for methyl and methine resonances, hexads for methylene resonances), the agreement between experimental and calculated chemical shift values is of the order of ±0.05−0.1 ppm; the relatively low resolution of the spectra makes it difficult to compare results for longer stereosequences.

When this comparison was attempted on the basis of higher-field ^{13}C NMR spectra like those of Figures 1 and 2, a first observation is that, in most cases, the separation between neighboring peaks is lower than 0.05 ppm.

Moreover, we have found that the relative chemical shift values are subjected to changes of up to 0.1 ppm when changing the solvent. As an example, Figure 3 shows the methyl region of two spectra of sample A, both recorded at 70 °C but using as a solvent 1,1,2,2-tetrachloroethane-d_2 in one case and cyclohexane-d_{12} in the other (note the slight improvement in resolution reached with the latter solvent); the relative chemical shifts of corresponding peaks are compared in Table 5. On the other hand, in all semiempirical calculations of chemical shifts of the type described above,[2c−1,7c] solvent effects on conformer populations are neglected.

Thus, it can be concluded that resonance assignment in high-field ^{13}C NMR spectra of polypropylene cannot rely exclusively on such predictive calculations, which can be taken only as a rough indication.

Table 1. Assignments of the Methyl and Methylene Resonances in the 150 MHz ^{13}C NMR Spectrum of Sample A (see Figures 1A and 2A), and Comparison between Experimental and Best-Fit Calculated Stereosequence Distribution

range/ peak no.	δ (exptl), ppm[a]	assignment	δ (calcd), ppm[a]	% fraction exptl	% fraction calcd[b]
		Methyl Resonances			
I	22.0−21.7	*mmmm*		40.0	40.8
1	21.94	*mmmmmmmm*	21.933 (20)		16.6
2	21.92	*mmmmmmmmrm*	21.899 (6)		5.3
3	21.89	*mmmmmmrr*	21.834 (15)		2.1
5	21.87	*mmmmmmmrmr*	21.819 (5)		1.3
6	21.84	*mmmmmmmrmm* +	21.811 (6)		5.3
		rmmmmmmrmm	21.798 (5)		1.3
8	21.82	*rmmmmmrm*	21.773 (13)		2.1
9	21.75	*mrmmmmrm*	21.685 (12)	1.0	1.0
II	21.7−21.4	*mmmr*		20.9	20.5
10	21.61	*mmmmmrrm*	21.660 (15)	1.8	2.1
13	21.58	*mmmmmrmr* +	21.596 (14)		2.1
		mmmmmrmm	21.574 (16)		8.4
14	21.56	*rmmmmrmm*	21.538 (12)		2.1
15	21.52	*rmmmrr* +	21.538 (32)	}	0.8
		rrmmmrmm +	21.474 (11)	} 1.8	0.5
		mrmmmrmr	21.472 (10)	}	0.5
16	21.49	*mrmmmrmm*	21.450 (12)	2.4	2.1
III	21.4−21.2	*rmmr*		2.5	2.6
20	21.30	*mrmmrr*	21.298 (31)		0.8
21	21.28	*mrmmrm*	21.230 (33)		1.7
IV	21.2−21.0	*mmrr*		4.7	5.2
22	21.13	*mmmrrm*	21.183 (39)	3.3	3.3
V	21.0−20.7	*mmrm* + *rmrr*		22.8	21.8
24	20.97	*mmmrmr*	21.030 (39)	3.2	3.3
25	20.91	*mmmmrmmr*	21.005 (14)	2.0	2.1
26	20.86	*mmmmrmmm* +	20.986 (16)		8.4
		rmmmrmmm	20.947 (13)		2.1
30	20.77	*mrmmrmmm*	20.848 (12)	2.1	2.1
VI	20.7−20.5	*rmrm*		4.8	5.2
31	20.67	*rrmrmr*	20.730 (28)	0.3	0.2
32	20.63	*rrmrmm*	20.672 (32)	1.0	0.8
33	20.60	*mrmrmr*	20.652 (31)	1.0	0.8
34	20.55	*mrmrmm*	20.592 (35)	2.5	3.3
VII+VIII	20.5−20.0	*rrrm* + *rrrr*		1.7	1.5
40	20.07	*mrrrmm*	20.083 (36)	0.6	0.8
IX	20.0−19.7	*mrrm*		2.5	2.6
45	19.80	*mmmrrmmr*	19.773 (14)	0.5	0.5
46	19.75	*mmmrrmmm*	19.743 (16)	1.1	1.0
		Methylene Resonances			
X	47.75−47.60	*mrmrm*		1.7	2.1
1	47.72	*mmmrmrmmm*	47.763 (12)		0.8
2	47.69	*mmrmrmr* +	47.679 (29)		0.7
		mmmrmrmmr	47.740 (11)		0.4
XI	47.60−47.42	*mrmrr*		1.1	1.0
4	47.51	*mmrmrrm*	47.498 (29)		0.7
XII	47.42−47.28	*rrmrr* + *mrrrm*		0.4	0.6
XIII	47.28−47.02	*mrrrr*		n.d.[c]	0.3
XIV	47.02−46.85	*rmmrm* + *rrrrr*		4.2	4.1
14	46.97	*mrmmrmm*	47.092 (29)		2.6
16	46.94	*mrmmrmr**	47.039 (26)		0.7
17	46.92	*rrmmrmm**	47.028 (27)		0.7
XV	46.85−46.58	*rmmrr* + *mmmrm* + *mmmrr*		20.8	21.5
19	46.86	*mrmmrrm*	46.889 (26)		0.7
20	46.84	*rmmmrmm*	46.864 (30)		2.6
24	46.78	*mmmmrmm*	46.773 (37)		10.5
25	46.73	*mmmmrmr*	46.725 (34)		2.6
29	46.62	*mmmmrrm*	46.586 (34)		2.6
XVI	46.58−46.40	*rmrrm*		0.7	1.0

Table 1 (Continued)

range/ peak no.	δ (exptl), ppm[a]	assignment	δ (calcd), ppm[a]	% fraction exptl	% fraction calcd[b]
XVII + XVIII	46.40−45.90	*rmmmr* + *mmmmr* + *mmrrm* + *rmrrr* + *mmmmm* + *mmrrr*		57.8	56.4
32	46.37	*mrmmmrm*	46.542 (27)		1.3
34	46.23	*mmmmmrm*	46.262 (35)		10.5
36	46.19	*rmmmmmr*	46.151 (29)		1.3
38	46.17	*mmmmmmr*	46.073 (13)		10.5
39	46.14	*mmmmmmmmr*	45.999 (13)		6.7
41	46.12	*mmmmmmmmm*	45.971 (16)		13.3
XIX	45.60−45.35	*rmrmr*		0.4	0.5
46	45.50	*mrmrmrm*	45.694 (42)		0.3
XX	45.35−45.10	*mmrmr*		4.2	4.1
49	45.19	*mmmrmrm*	45.281 (52)		2.6
XXI	45.10−44.80	*mmrmm*		8.7	8.2
50	44.97	*mmmrmmr*	44.982 (53)		2.6
51	44.87	*mmmrmmm*	44.867 (62)		5.2

best-fit value of the adjustable parameter in the calculations of stereosequence distribution: $P(m) = 1 - P(r) = 0.79_9$

[a] Downfield of TMS. [b] According to the chain-end statistical model. [c] n.d. = not detected.

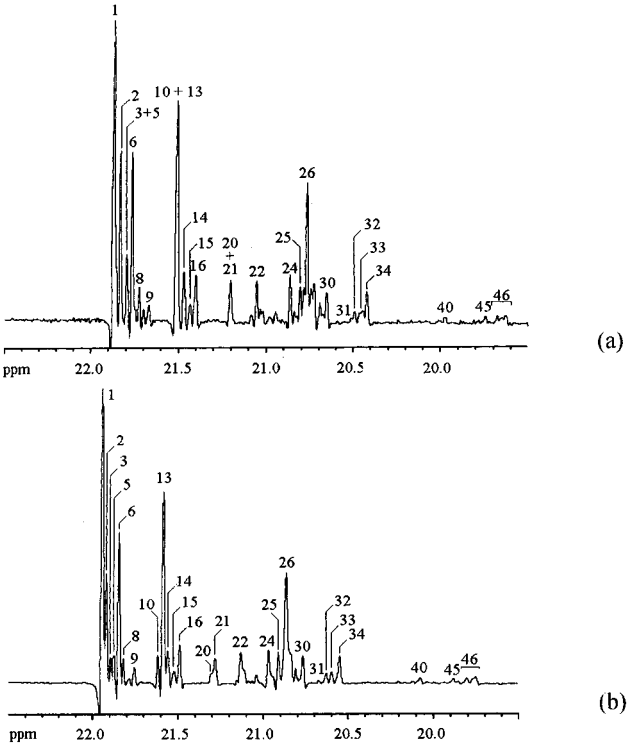

Figure 3. Methyl region of the 150 MHz ^{13}C NMR spectra of sample A, dissolved at 70 °C in cyclohexane-d_{12} (a) and 1,1,2,2-tetrachloroethane-d_2 (b); δ scale is in ppm downfield of TMS. The relative chemical shift values of corresponding peaks in the two spectra are compared in Table 5.

In this respect, it is worth recalling that empirical rules *which do not require calculations* for sequencing methyl and methylene resonances in the ^{13}C NMR spectra of polypropylene were formulated long ago by Ferro *et al.*[2f] What follows is a rephrased version which makes use of current stereochemical notations:

Rule 1 (methyl). Let us divide the four steric *n*ads (*n* even) centered on a given (n − 2)ad in two hemistereosequences. The *n*ad with both hemistereosequences containing an even number of *r* diads will be the one occurring at lower field; the *n*ad with both hemistereosequences containing an odd number of *r* diads will be the one occurring at higher field. Nothing can be said about the relative ordering of the remaining two *n*ads, apart from a tendency to show close values of chemical shift.

Rule 2 (methylene). Let us consider the four steric *n*ads (*n* odd) centered on a given (n − 2)ad. The four (n − 1)ads obtained by dropping the central diad can be divided in two hemistereosequences, for which a rule opposite to rule 1 holds.

Rule 3 (methylene). Of two *n*ads (*n* odd) differing *only* for the central diad, the one centered on a *m* diad will occur at lower field.

It should be noted that methylene chemical shifts can be considered the result of a "side effect" (rule 2) and of a "center effect" (rule 3); their delicate balance makes the methylene region of the spectrum by far richer in peak overlaps than the methyl region.

The Assignment Procedure. Moving from these considerations, the following protocol for resonance assignment in the spectra of Figures 1 and 2 was established:

Step 1. The degree of stereoregularity of each model polymer was preliminarily evaluated from the methyl pentad distribution, with a best-fit procedure in terms of the appropriate statistical model.

In spite of the low number of experimental data (≤9), this approach was adopted since no overlap occurs between resonances associated with different pentads (with the well-known[2,3] exception of the *mmrm* and *rmrr* ones); the corresponding nine resonance ranges (denoted as I−IX in Figure 1) could thus be recognized on inspection and the pertinent integrals measured with high accuracy.

In this starting phase, the analysis was not extended to the methylene region, due to large overlaps between peaks corresponding to different hexads.

For each polymer sample, once the best-fit values for the adjustable parameters in the statistical set of equations were determined, it was possible to calculate the probability of occurrence for stereosequences of any length.

The matrix multiplication methods adopted for such calculations have already been described in the Appendix to ref 3f. Matrixes **C** (for chain-end control[6]), **E**

Table 2. Assignments of the Methyl and Methylene Resonances in the 150 MHz ^{13}C NMR Spectrum of Sample B (see Figures 1B, 2B), and Comparison between Experimental and Best-Fit Calculated Stereosequence Distribution

range/ peak no.	δ (exptl), ppm[a]	assignment	δ (calcd), ppm[a]	% fraction exptl	% fraction calcd[b]
		Methyl Resonances			
I	22.0−21.7	*mmmm*		34.8	34.9
1	21.94	*mmmmmm*	21.900 (52)	23.3	22.9
3	21.89	*mmmmmr*	21.805 (44)		10.8
7	21.83	*rmmmmr*	21.71 (36)		1.3
II	21.7−21.4	*mmmr*		16.3	16.6
10	21.61	*mmmmrr*	21.634 (40)	11.2	10.7
15	21.56	*rmmmrr*	21.538 (32)		2.5
III	21.4−21.2	*rmmr*		2.6	2.4
17	21.32	*mrrmmrrm*	21.385 (10)		0.8
IV	21.2−21.0	*mmrr*		16.3	16.6
22	21.13	*mmmrrm* + *mmmrrr**	21.183 (39) 21.137 (37)	13.1	10.7 2.5
23	21.08	*rmmrrm** + *rmmrrr*	21.082 (31) 21.035 (29)	3.2	2.5 0.7
V	21.0−20.7	*mmrm* + *rmrr*		9.3	9.5
24	20.97	*mmmrmr*	21.030 (39)		2.5
27	20.83	*rrmrrm*	20.896 (28)		2.5
VI	20.7−20.5	*rmrm*		3.5	4.7
34	20.55	*mrmrmm*	20.592 (35)		2.5
VII	20.5−20.25	*rrrr*		2.7	2.4
35	20.38	*mrrrrm*	20.358 (30)	1.1	1.3
VIII	20.25−20.0	*rrrm*		5.2	4.7
40	20.08	*mrrrrmmr*	20.021 (10)	0.4	
41	20.04	*rrrrrmmm* + *mrrrrmmm*	20.013 (11) 19.994 (12)	2.1	0.4 1.6
IX	20.0−19.7	*mrrm*		9.3	8.3
43	19.84	*mmrrmr*	19.854 (37)	3.1	2.5
45	19.79	*mmmrrmmr*	19.773 (14)	6.2	1.6
46	19.76−19.75	*mmmrrmmm*	19.743 (16)		3.5
		Methylene Resonances			
X	47.75−47.60	*mrmrm*		0.8	1.6
1	47.72	*mmmrmrmmm*	47.763 (12)		0.7
XI	47.60−47.42	*mrmrr*		0.6	1.5
XII	47.42−47.28	*rrmrr* + *mrrrm*		1.8	2.4
7	47.35	*mrrmrrm*	47.271 (25)		1.0
XIII	47.28−47.02	*mrrrr*		3.3	3.3
9	47.19	*mmrrrrm*	47.149 (42)		2.0
XIV	47.02−46.85	*rmmrm* + *rrrrr*		1.5	2.2
XV	46.85−46.58	*rmmrr* + *mmmrm* + *mmmrr*		17.5	19.9
23	46.79	*rrmmrrm*	46.828 (24)		2.0
28	46.66	*rmmmrrm* + *mmmmrrr*	46.672 (27) 46.628 (32)		2.0 2.0
29	46.62	*mmmmrrm*	46.586 (34)		8.7
XVI	46.58−46.40	*rmrrm*		4.5	3.3
30	46.51	*rrmrrmm*	46.537 (43)		2.0
XVII	46.40−46.08	*rmmmr* + *mmmmr* + *mmrrm* + *rmrrr* + *mmmmm*		58.8	57.9
38	46.19	*mmmmmmr*	46.073 (35)		8.7
39	46.15	*mmmmmmmmr*	45.999 (13)		5.7
41	46.12	*mmmmmmmmm*	45.971 (12)		12.2
XVIII	46.08−45.90	*mmrrr*		7.6	3.3
XIX	45.60−45.35	*rmrmr*		1.0	0.7

Table 2 (Continued)

range/ peak no.	δ (exptl), ppm[a]	assignment	δ (calcd), ppm[a]	% fraction exptl	% fraction calcd[b]
XX	45.35−45.10	*mmrmr*		2.0	3.3
49	45.19	*mmmrmrm*	45.281 (52)		2.0
XXI	45.10−44.80	*mmrmm*		0.7	0.7

best-fit value of the adjustable parameter in the calculations of stereosequence distribution: $\sigma = 0.81$

[a] Downfield of TMS. [b] According to the enantiomorphic-site statistical model.

(for enantiomorphic-site control[5]), and $\mathbf{A_{CM}}$ (for chain-migratory syndiotactic control[16]) were used for samples A, B, and C respectively.

The case of hemiisotactic polypropylene (sample D), not treated in ref 3f, is more complex. This polymer was prepared for the first time in 1982 by Farina and co-workers by hydrogenation of isotactic *trans*-1,4-poly(2-methyl-pentadiene) with *p*-toluenesulfonyl hydrazide;[17a] however, with the advent of group 4 metallocene catalysts,[1c] it is now possible to obtain hemiisotactic polypropylene directly from propene polymerization.

A suitable catalyst precursor is, *e.g.*, Me_2C(3-Me-cyclopentadienyl)(9-fluorenyl)$ZrCl_2$[18] (Chart 2d). The cationic active species formed by activation with an appropriate co-catalyst (*e.g.*, MAO) has two diastereotopic coordination sites available for the monomer and the growing polymer chain: propene insertion is almost completely enantioselective when it occurs at the more hindered of the two sites (site 1 in Chart 1d), whereas it is almost perfectly non-enantioselective in the other case (site 2 in Chart 1d).[18,22,23]

The resulting polymer is hemiisotactic due to the "chain migratory" propagation mechanism,[16,18] the incoming monomer, and the polymer chain exchanging regularly at each insertion step between the two sites.

A rigorous description of chain propagation requires a statistical model with four adjustable parameters: σ_1 and σ_2, probability of monomer insertion with a given enantioface at site 1 and site 2, respectively; P_{12} and P_{21}, probability of monomer insertion at site 2 after a previous insertion at site 1 and *vice versa*.

The conditional probabilities of all possible insertion events are given by the following matrix:

$$\mathbf{A_{HIT}} = \begin{array}{c|cccc} & S_1 & R_1 & S_2 & R_2 \\ \hline \boldsymbol{S_1} & \sigma_1(1-P_{12}) & (1-\sigma_1)(1-P_{12}) & \sigma_2 P_{12} & (1-\sigma_2)\,P_{12} \\ \boldsymbol{R_1} & \sigma_1(1-P_{12}) & (1-\sigma_1)(1-P_{12}) & \sigma_2\,P_{12} & (1-\sigma_2)\,P_{12} \\ \boldsymbol{S_2} & \sigma_1\,P_{21} & (1-\sigma_1)P_{21} & \sigma_2(1-P_{21}) & (1-\sigma_2)\,(1-P_{21}) \\ \boldsymbol{R_2} & \sigma_1\,P_{21} & (1-\sigma_1)P_{21} & \sigma_2(1-P_{21}) & (1-\sigma_2)\,(1-P_{21}) \end{array}$$

with rows indexed to the chirality (*S* or *R*) of the last-inserted monomeric unit in the growing chain and columns indexed to the chirality of the new unit to be generated. The subscripts 1 and 2 refer, for the rows, to the site where the last monomeric unit was inserted, and for the columns, to that where the new unit is being inserted. As an example, the element [11] of $\mathbf{A_{HIT}}$ is the conditional probability of two consecutive insertions at site 1 leading to two monomeric units with the same *S* configuration.

This four-parameter statistical model cannot be applied in a significant way to the pentad distribution; therefore, preliminary calculations were performed using the matrix which corresponds to *ideal* hemiisotactic propagation, with $\sigma_1 = 1$, $\sigma_2 = 0.5$, $P_{12} = P_{21} = 1$.

Step 2. Peak assignments were then operated on the basis of rules 1−3 for the prediction of the chemical shift sequence[2f] and of a comparison between observed and calculated integrals.

For the (predominantly) isotactic and syndiotactic polymer samples, it was trivial to assign the intense peaks corresponding to configurational sequences with up to one stereoerror; from this start, it was then possible to assign unambiguously the weaker resonances associated with stereosequences containing two and—in some cases—three stereoerrors.

The case of hemiisotactic polypropylene, on the other hand, was highly facilitated by the stringent selection rules of stereosequence generation and by the availability of detailed methyl resonance assignments published by Farina and co-workers.[17]

A careful cross check was then performed on all four spectra, looking for correspondence between peaks assigned to the same stereosequence.[24]

The final list of assignments for the methyl resonances (mostly at heptad/nonad levels) and for the methylene resonances (mostly at octad/decad levels) is given in column 3 of Tables 1−4.

Step 3. Calculations of chemical shifts within the *γ-gauche* approximation[7c] using the RIS model of Suter and Flory[21] and Tonelli's scheme for the γ parameters[2g] were performed (column 4 of Tables 1−4).

In consideration of the very high number of available resonances, the numerical values of δ_0 and γ to be used in eq 1 were redetermined by a least-squares multiple regression:

$$\delta_0(CH_3) = 27.07 \pm 0.06 \text{ ppm}, \gamma(CH_3) = -5.24 \pm 0.06 \text{ ppm}$$

$$\delta_0(CH_2) = 49.18 \pm 0.04 \text{ ppm}, \gamma(CH_2) = -3.97 \pm 0.05 \text{ ppm}$$

The above two γ values are very close to those reported by Tonelli[2g] ($\gamma(CH_3) = -5.3$ ppm; $\gamma(CH_2) = -3.7$ ppm). A slightly lower $\gamma(CH_2)$ seems in better agreement with results of cross polarization magic angle spinning (CP/MAS) ^{13}C NMR;[7b] on the other hand, it should be noted that Tonelli's estimate was made on experimental data collected over a large temperature interval (20−140 °C), whereas the one in the present investigation refers to a single temperature (70 °C).

It is well-known that, for relatively short stereosequences, chemical shift values are somewhat sensitive to their steric environment.[2c−l,7c] To keep trace of the finite length of each given *n*ad, its calculated δ value was expressed as the average of those corresponding to the two $(n + p)$ads at higher and lower field according to rules 1−2[2f], with *p* high enough to reach convergence (typically, $(n + p) \approx 20$); the half-difference between such two values, which represents the maximum error on the predicted chemical shift value attributable to the steric environment, is reported in parentheses.

Table 3. Assignments of the Methyl and Methylene Resonances in the 150 MHz ^{13}C NMR Spectrum of Sample C (see Figures 1C and 2C), and Comparison between Experimental and Best-Fit Calculated Stereosequence Distribution

range/ peak no.	δ (exptl), ppm[a]	assignment	δ (calcd), ppm[a]	% fraction exptl	% fraction calcd[b]
		Methyl Resonances			
I	22.0−21.7	*mmmm*		n.d.[c]	0.3
II	21.7−21.4	*mmmr*		1.9	2.0
15	21.54	*rmmmrr*	21.538 (32)		1.2
III	21.4−21.2	*rmmr*		2.9	3.1
19	21.29	*rrmmrr*	21.366 (28)		2.0
IV	21.2−21.0	*mmrr*		5.9	6.5
23	21.06	*rmmrrr*	21.035 (29)	4.1	3.9
V	21.0−20.7	*mmrm* + *rmrr*		20.2	20.5
27	20.86	*rrrmrrmr*	20.876 (8)	1.9	1.8
28	20.83	*rrmrrr*	20.846 (26)		12.0
29	20.78	*rmrmrrrr*	20.792 (8)	2.0	1.8
VI	20.7−20.5	*rmrm*		5.5	4.8
31	20.68	*rrmrmr*	20.730 (28)	3.3	2.8
32	20.64	*rrmrmm*	20.672 (32)		1.0
33	20.61	*mrmrmr*	20.652 (31)		0.7
VII	20.5−20.25	*rrrr*		40.3	40.1
35	20.40	*mrrrrm*	20.358 (30)	1.4	1.6
36	20.34	*mrrrrr*	20.298 (28)	12.0	12.9
37	20.29	*rrrrrr*	20.236 (25)	26.9	25.6
VIII	20.25−20.0	*rrrm*		20.0	20.2
38	20.20	*mrrrmr*	20.156 (31)	3.0	3.0
39	20.14	*rrrrmr*	20.090 (28)	12.5	12.0
40	20.08	*mrrrmm* +	20.083 (36)	}	1.1
		rrrrrmmr +	20.040 (9)	4.5	2.5
		mrrrrmmr	20.021 (10)	}	0.6
IX	20.0−19.7	*mrrm*		3.2	2.6
42	19.98	*rmrrmr*	19.934 (31)	2.0	1.4
43	19.91	*mmrrmr*	19.854 (37)	1.0	1.0
		Methylene Resonances			
X	47.75−47.60	*mrmrm*		0.6	0.5
3	47.64	*rmrmrmr*	47.616 (24)		0.3
XI	47.60−47.42	*mrmrr*		4.1	3.8
5	47.49	*rmrmrrr*	47.492 (23)		2.3
XII	47.42−47.28	*rrmrr* + *mrrrm*		8.5	9.5
6	47.36	*rrrmrrr*	47.373 (21)		4.8
XIII	47.28−47.02	*mrrrr*		15.6	16.1
9	47.20	*mmrrrrr*	47.222 (39)		3.3
11	47.14	*rmrrrrr*	47.131 (33)		9.6
12	47.09	*rmrrrrm*	47.058 (36)		2.4
XIV	47.02−46.85	*rmmrm* + *rrrrr*		32.2	33.3
13	46.98	*mrrrrrrrr*	46.953 (10)		6.6
15	46.94	*rrrrrrrrr*	46.932 (9)		13.0
18	46.88	*rmrrrrrrr* +	46.882 (9)		6.1
		mmrrrrrrr	46.856 (11)		2.1
XV	46.85−46.58	*rmmrr* + *mmmrm* + *mmmrr*		8.0	6.9
21	46.84	*rrmmrrr*	46.872 (22)		3.2
26	46.71	*rmmmrrr*	46.715 (25)		1.0
XVI	46.58−46.40	*rmrrm*		4.7	3.8
30	46.50	*rrmrrmm*	46.537 (43)		0.8
31	46.43	*rrmrrmr*	46.441 (36)		2.2
XVII	46.40−46.08	*rmmmr* + *mmmmr* + *mmrrm* + *rmrrr* + *mmmmm*		18.1	17.6
33	46.25	*mrmrrrr*	46.336 (36)		2.4
35	46.21	*rrmrrrr*	46.253 (34)		9.6
40	46.13	*rrmrrrm*	46.175 (37)		2.4

Table 3 (Continued)

range/ peak no.	δ (exptl), ppm[a]	assignment	δ (calcd), ppm[a]	% fraction exptl	% fraction calcd[b]
XVIII	46.08−45.90	*mmrrr*		5.1	5.2
43	46.02	*rmmrrrr*	46.046 (38)		3.1
XIX	45.60−45.35	*rmrmr*		1.9	1.8
47	45.48	*rrmrmrr*	45.523 (36)		1.1
XX	45.35−45.10	*mmrmr*		1.2	1.2
48	45.25	*rmmrmrr*	45.310 (40)		0.7
XXI	45.10−44.80	*mmrmm*		n.d.[c]	0.2

best-fit values of the adjustable parameters in the calculations of stereosequence distribution: $\sigma = 0.97_6$ $P_{sk} = 0.18_3$

[a] Downfield of TMS. [b] According to the chain-migratory syndiotactic statistical model. [c] n.d. = not detected.

It is important to note that these calculations were *not* used for resonance assignment, with the only exception of couples of adjacent peaks associated with *equiprobable* steric *n*ads whose chemical shift sequence cannot be decided in terms of rules 1−3[2f] and/or by comparative analysis of the four different spectra. In such cases (fortunately very limited in number and marked with asterisks in Tables 1−4) the only possible hint for deciding "which is which" is provided by the predicted value of the chemical shift; in view of the discussed limitations of such predictions, these assignments should be regarded as dubious.

In general, the agreement between experimental and calculated chemical shift values is decent, as the standard deviations (0.05 ppm for the methyl resonances, 0.07 ppm for the methylene resonances) indicate.

Step 4. For each spectrum, a second best-fit calculation was performed on the experimental normalized integrals of both methyl and methylene resonances (columns 5 and 6 of Tables 1−4).

The methylene region was divided in 12 ranges (denoted as X−XXI in Figure 2) corresponding to the 20 different steric hexads (some of which inextricably overlapped: two in each of ranges XII and XIV; three in range XV; five in range XVII), by analogy to what had already been done for the methyl region.

The two sets of normalized methyl and methylene integrals, including *all* possible pentads and hexads, respectively, were fed to the best-fit program although they are not statistically independent, in order to reduce the experimental error (see Experimental Section).

Concerning the use of longer stereosequences, it is important to note that, under the adopted experimental conditions, it turned out to be impossible to locate peaks associated with steric *n*ads representing less than 0.5% (indicatively) of the total methyl or methylene integral.[25] This represents a complication in the best-fit calculations, since: (i) the cumulative integral of such weak resonances is significant (10−20% of the total one) and contributes in an unpredictable way to the integrals of the more intense, assigned peaks; (ii) the possibility of rigorous procedures of peak deconvolution, which would require a complete resonance assignment at the undecad/tridecad level for the methyl region and at the decad/dodecad level for the methylene region (unfeasible even at 150 MHz), is precluded.

In view of the above, we decided to include in the best-fit only those individual peaks or aggregates of peaks for which *all* contributions to the integral could be identified (column 5 of Tables 1−4). For samples A−C, in particular, such a condition was satisfied only for part of the methyl peaks; however, in spite of this rather conservative procedure, 20−30 statistically independent integrals for each sample could be used in the calculations.

The theoretical integrals of all assigned resonances (including those not used in the best-fit procedures, for a visual comparison with the observed intensities in the spectra of Figures 1 and 2) were calculated (column 6 of Tables 1−4).

The agreement with the experimental data is good for samples A, C, and D. In contrast, some discrepancies can be noted for sample B, mostly on the methylene resonances, due to the relatively low regioregularity (1.1 mol % of 3,1 monomer enchainments[26]) and average molecular mass ($M_n = 3.3 \times 10^3$ amu) of this sample; indeed, for a correct application of the statistical model of chain propagation, the best-fit analysis should be restricted to fully regioregular sequences far from the chain ends. In the methyl region of the spectrum of sample B (Figure 1B), it was possible to locate most resonances of sequences not corresponding to these specifications[4e,g,26] and to exclude them from the normalization; however, this procedure could not be applied to the much more crowded methylene region (Figure 2B), for which uncorrected data had to be used.

We note that, for samples A−C, the best-fit values of the adjustable parameters obtained at step 4 (and reported in Tables 1−3) do not differ significantly from those evaluated at step 1 from the methyl pentad distribution only; this is not surprising, in view of the very simple configurational statistics of these polymers.

For sample D, the following values of the four adjustable parameters were deduced from the best-fit of the complete stereosequence distribution (Tab. 4): $\sigma_1 = 0.99$, $\sigma_2 = 0.47$, $P_{12} = P_{21} = 1.00$. Such values indicate only slight deviations from the ideal case, which account however for the observation of low amounts of "prohibited"[17] stereosequences (*e.g.*, *mmrm* + *rmrr*, *rmrm*), as well as of small differences in the concentration of stereosequences that, in an ideally hemiisotactic polymer, should occur with equal probability[17] (Figures 1D and 2D and Table 4).

Conclusions

The assignments of the methyl and methylene regions in the 150 MHz ^{13}C NMR spectra of polypropylene samples of various tacticities reported in the previous section constitute an experimental basis that can be used for refining and testing theoretical methods of chemical shift predictions as well as for in-depth statistical analyses of polymer configuration.

In this latter respect, we will illustrate in forthcoming papers the improvements derived by the use of these

Table 4. Assignments of the Methyl and Methylene Resonances in the 150 MHz ^{13}C NMR Spectrum of Sample D (see Figures 1D and 2D), and Comparison between Experimental and Best-Fit Calculated Stereosequence Distribution

range/ peak no.	δ (exptl), ppm[a]	assignment	δ (calcd), ppm[a]	% fraction exptl	% fraction calcd[b]
		Methyl Resonances			
I	22.0−21.7	*mmmm*		16.0	16.3
1	21.94	*mmmmmmmm* +	21.933 (20)		3.6
		mmmmmmmmrr +	21.908 (6)	6.8	2.6
		rrmmmmmmrr	21.871 (4)		1.4
3	21.89	*mmmmmmmmrrmm* +	21.847 (2)		1.2
		*mmmmmmmmrrrr**	21.839 (2)		1.3
4	21.88	*rrmmmmmmrrmm** +	21.833 (1)	4.9	1.3
		rrmmmmmmrrrr	21.825 (1)		1.4
7	21.84	*rrmmmmrr*	21.734 (10)	4.3	3.0
II	21.7−21.4	*mmmr*		12.5	11.9
10	21.61	*mmmmmmrrmm*	21.669 (5)		2.6
11	21.60	*mmmmmmrrrr* +	21.649 (5)		2.8
		rrmmmmrrmm	21.632 (4)		2.8
12	21.59	*rrmmmmrrrr*	21.612 (3)		3.1
III	21.4−21.2	*rmmr*		6.4	6.5
17	21.34	*mmrrmmrrmm*	21.391 (4)		1.4
18	21.31	*mmrrmmrrrr*	21.371 (3)		3.1
19	21.30	*rrrrmmrrrr*	21.351 (2)		1.7
IV	21.2−21.0	*mmrr*		25.6	24.5
22	21.12	*mmmmrrmm* +	21.208 (14)	12.3	5.4
		*mmmmrrrr**	21.161 (13)		5.9
23	21.07	*rrmmrrmm** +	21.103 (10)	13.3	5.9
		rrmmrrrr	21.055 (8)		6.5
V	21.0−20.7	*mmrm* + *rmrr*		1.2	0.9
VI	20.7−20.5	*rmrm*		0.6	0.5
VII	20.5−20.25	*rrrr*		19.7	20.3
35	21.38	*mmrrrrmm*	20.378 (11)	3.8	3.0
36	20.33	*mmrrrrrr*	20.317 (9)	6.5	6.5
37	20.29	*rrrrrr*	20.236 (25)	9.4	10.5
VIII	20.25−20.0	*rrrm*		11.3	13.1
40	20.08	*rrrrrrmmrr* +	20.034 (3)	5.8	3.4
		*mmrrrrmmrr**	20.014 (3)		3.1
41	20.04	*rrrrrrmmmm** +	20.006 (4)	5.5	3.1
		mmrrrrmmmm	19.986 (4)		2.8
IX	20.0−19.7	*mrrm*		6.7	5.9
44	19.85	*rrmmrrmmrr*	19.795 (3)	2.0	1.5
45	19.81	*mmmmrrmmrr*	19.764 (5)	4.7	2.8
46	19.76−19.75	*mmmmrrmmmm*	19.733 (6)		1.3
		Methylene Resonances			
X	47.75−47.60	*mrmrm*		n.d.[c]	0.1
XI	47.60−47.42	*mrmrr*		n.d.[c]	0.2
XII	47.42−47.28	*rrmrr* + *mrrrm*		n.d.[c]	0.2
XIII	47.28−47.02	*mrrrr*		14.2	12.8
8	47.24	*mmmrrrrrr*	47.226 (13)	3.0	3.1
9	47.20	*rmmrrrrrr* +	47.193 (10)	6.8	3.4
		mmmrrrrmm	47.152 (15)		2.8
10	47.16	*rmmrrrrmm*	47.119 (13)	4.4	3.1
XIV	47.02−46.85	*rmmrm* + *rrrr*		13.9	14.2
13	46.98	*mrrrrrrr*	46.953 (10)	3.1	3.4
15	46.93	*rrrrrrrr* +	46.932 (9)	6.9	3.7
		mmrrrrrrm	46.878 (12)		3.1
18	46.90	*mmrrrrrrr*	46.856 (11)	3.9	3.4
XV	46.85−46.58	*rmmrr* + *mmmrm* + *mmmrr*		25.6	24.7
21	46.84	*rrrmmrrrr*	46.875 (6)		3.4
22	46.82	*mrrmmrrrr*	46.857 (7)		3.1
23	46.79	*rrrmmrrmm* +	46.830 (8)		3.1
		mrrmmrrmm	46.812 (8)		2.8
27	46.69	*rmmmmrrrr*	46.639 (9)	3.7	3.1
28	46.66	*mmmmmrrrr* +	46.607 (11)	9.5	2.8
		rmmmmrrmm	46.596 (10)		2.8
29	46.63	*mmmmmrrmm*	46.564 (13)		2.6

Table 4 (Continued)

range/ peak no.	δ (exptl), ppm[a]	assignment	δ (calcd), ppm[a]	% fraction exptl	% fraction calcd[b]
XVI	46.58−46.40	*rmrrm*		n.d.[c]	0.2
XVII	46.40−46.08	*rmmmr* + *mmmmr* + *mmrrm* + *rmrrr* + *mmmmm*		33.1	34.2
37	46.18	*rrmmmmmmr*	46.079 (10)		2.8
39	46.15	*mmmmmmmrr* + *mmmmmmmmr*	46.050 (12) 45.999 (14)		2.6 2.6
41	46.12	*mmmmmmmmm*	45.932 (23)		2.3
XVIII	46.08−45.90	*mmrrr*		13.2	12.8
42	46.05	*rrmmrrrrm*	46.041 (12)	3.4	3.1
43	46.02	*rrmmrrrrr*	46.019 (11)	3.7	3.4
44	45.98	*mmmmrrrrm*	45.924 (17)	6.1	2.8
45	45.96	*mmmmrrrrr*	45.902 (16)		3.1
XIX	45.60−45.35	*rmrmr*		n.d.[c]	0.1
XX	45.35−45.10	*mmrmr*		n.d.[c]	0.2
XXI	45.10−44.80	*mmrmm*		n.d.[c]	0.1

best-fit values of the adjustable parameters in the calculations of stereosequence distribution:
$\sigma_1 = 0.99$ $\sigma_2 = 0.47_7$ $P_{12} = 1.00$ $P_{21} = 1.00$

[a] Downfield of TMS. [b] According to the chain-migratory hemiisotactic statistical model. [c] n.d. = not detected.

Table 5. Comparison between the Relative Chemical Shift Values of Corresponding Peaks in the Methyl Region of the 150 MHz ^{13}C NMR Spectra of Sample A at 70 °C in 1,1,2,2-Tetrachloroethane-d_2 and Cyclohexane-d_{12} (see Figure 3)[a]

peak no.	assignment	$\Delta\delta$ (exptl), ppm: 1,1,2,2-tetrachloroethane-d_2	$\Delta\delta$ (exptl), ppm: cyclohexane-d_{12}
1	*mmmmmmmm*	0.00	0.00
2	*mmmmmmmmrm*	−0.02	−0.04
3	*mmmmmmrr*	−0.05	−0.08
5	*mmmmmmmrmr*	−0.07	−0.08
6	*mmmmmmmrmm* + *rmmmmmmrmm*	−0.10	−0.11
8	*rmmmmmrm*	−0.12	−0.15
9	*mrmmmmrm*	−0.19	−0.20
10	*mmmmmrrm*	−0.33	−0.36
13	*mmmmmrmr* + *mmmmmrmm*	−0.36	−0.36
14	*rmmmmrmm*	−0.38	−0.40
15	*rmmmrr* + *rrmmmrmm* + *mrmmmrmr*	−0.42	−0.44
16	*mrmmmrmm*	−0.45	−0.47
20	*mrmmrr*	−0.64	−0.67
21	*mrmmrm*	−0.66	−0.67
22	*mmmrrm*	−0.81	−0.82
24	*mmmrmr*	−0.97	−1.00
25	*mmmmrmmr*	−1.03	−1.06
26	*rmmmrmmm* + *mmmmrmmm*	−1.08	−1.08 −1.10
30	*mrmmrmmm*	−1.17	−1.21
31	*rrmrmr*	−1.27	−1.35
32	*rrmrmm*	−1.31	−1.37
33	*mrmrmr*	−1.34	−1.43
34	*mrmrmm*	−1.39	−1.45
40	*mrrrmm*	−1.87	−1.90
45	*mmmrrmmr*	−2.14	−2.13
46	*mmmrrmmm*	−2.19	−2.22

[a] The δ scale is referred to the *mmmmmmmm* nonad, set at $\delta = 0$ ppm.

high-field ^{13}C NMR data in the investigation of complex cases such as those represented by polypropylenes produced with multisite or oscillating Ziegler−Natta catalysts.

The spectra in Figures 1 and 2 have been obtained under conditions (see Experimental Section) chosen so as to represent a compromise between the conflicting requirements for good polymer solubility, reasonable signal-to-noise ratio, and maximum resolution. In particular, highly dilute polymer solutions were used, in order to avoid any resonance broadening due to entangling effects[27] and to be able to dissolve all four model polymer samples at a temperature as low as 70 °C. In addition, the FIDs were collected with a size of 64K points/scan, corresponding to a digital resolution of 0.2 Hz, which allows one to take full profit from the chemical shift spreading in the ^{13}C spectrum.[28]

Of course, appreciable changes in the fine structure of the ^{13}C NMR spectra shown in this paper are to be expected if the acquisition conditions need to be changed for some reason (*e.g.*, higher temperature required for dissolving high-melting samples). However, at least the protocol used for resonance assignment should represent a guideline of general validity for subsequent studies on further polymer structures.

Experimental Section

Polymer Preparation. The polymerizations were run in a magnetically stirred (1000 rpm) 300 mL stainless steel reactor (Brignole AU-300). The appropriate amounts of MAO (Witco, 10% by weight solution in toluene) and of a catalyst solution in anhydrous toluene were charged in the reactor, thermostated at the chosen temperature, and saturated with propene. The reaction was allowed to proceed at constant monomer concentration for a given time, after which it was stopped by monomer degassing. The polymers were coagulated in methanol (500 mL) acidified with HCl (aqueous, concentrated; 10 mL), filtered, washed with methanol, and vacuum-dried (6 h at 15 mbar and 60 °C).

The following conditions were used:

Sample A: Bis(cyclopentadienyl)$TiCl_2$ (Witco), 14 μmol in 20 mL of toluene; MAO solution, 1.0 mL; $T = -20$ °C; propene, 50 g; polymerization time, 12 h. Yield, 15 g.

Sample B: *rac*-Ethylenebis(4,5,6,7-tetrahydro-1-indenyl)-$ZrCl_2$ (Witco), 1.0 μmol in 20 mL of toluene; MAO solution, 3.0 mL; $T = 50$ °C; partial pressure of propene, constant at 0.7 bar; polymerization time, 1 h. Yield, 7 g.

Sample C: Me_2C(cyclopentadienyl)(9-fluorenyl)$ZrCl_2$, 2.5 μmol in 50 mL of toluene; MAO solution, 2.1 mL; $T = 80$ °C; partial pressure of propene, constant at 1.5 bar; polymerization time, 40 min. Yield, 2.8 g.

^{13}C NMR Characterization. $^{13}C\{^1H\}$ NMR spectra were run on a Bruker AMX-600 spectrometer operating at 150.9 MHz on dilute (<5 mg/mL) polymer solutions in 1,1,2,2-tetrachloroethane-d_2 or—occasionally—in cyclohexane-d_{12} at 70.0 °C.

A 2 s relaxation delay with a 2.3 s acquisition time and a pulse angle of ≈45° were applied, so as to attain conditions far from any saturation but close enough to the maximum signal-to-noise ratio.[29] Proton broad-band decoupling was achieved with the GARP sequence.[30] Due to the high number of resonances, at least 25K scans were collected with 64K points/scan.

After zero filling, Fourier transformation was performed either without any further correction or after the application of a weak resolution-enhancing Gaussian function.

It has been shown[31,32] that spin—lattice relaxations are very similar for chemically equivalent groups differing only for the tacticity, so that all resonances of CH_3 and CH_2 groups in fully regioregular polypropylene sequences (far from the chain ends) have basically the same nuclear Overhauser effect (NOE). Quantitative data of stereosequence distributions can thus be obtained from an accurate resonance integration. Note that the spectra shown in Figures 1—3 were resolution-enhanced, whereas only zero filling followed by Fourier transformation was applied in the case of spectra to be used for resonance integration.

From repeated measurements on independent spectra of the same polymer sample, it was estimated that the uncertainty on the normalized peak areas A_i is of the order of $\pm 0.05A_i$ for $A_i > 5\%$ and of $\pm 0.25\%$ for $A_i < 5\%$.

The best-fit calculations of stereosequence distributions were performed with the CONFSTAT program (M. Vacatello, University of Naples).

Acknowledgment. The authors wish to thank Mr. E. Rossi (NMR Service, CNR Research Area, Rome) for expert technical assistance in the NMR experiments, Dr. C. J. Schaverien (Shell Research and Technology Centre, Amsterdam) for the preparation of a sample of Me_2C(cyclopentadienyl)(9-fluorenyl)$ZrCl_2$, Professor G. Di Silvestro (University of Milan) for kindly providing a sample of hemiisotactic polypropylene, and Witco GmbH (Bergkamen, FRG) for donating samples of metallocenes and MAO. Financial assistance from the Italian Ministry for the University and from the National Research Council of Italy (CNR, Progetto Strategico "*Materiali Polimerici Innovativi*") is acknowledged.

References and Notes

(1) Reviews on the stereochemistry of transition metal catalyzed 1-alkene polymerizations: (a) Corradini, P.; Busico, V.; Guerra, G. *Comprehensive Polymer Science*; Pergamon Press: Oxford, 1988; Vol. 4, pp 29—50. (b) Pasquon, I.; Porri, L.; Giannini, U. *Stereoregular Linear Polymers*. In *Encyclopedia of Polymer Science and Engineering*, 2nd ed.; Wiley-Interscience: New York, 1989; Vol. 15, pp 632—763. (c) Brintzinger, H. H.; Fischer, D.; Mülhaupt, R.; Rieger, B.; Waymouth, R. M. *Angew. Chem., Int. Ed. Engl.* **1995**, *34*, 1143.

(2) Resonance assignment in ^{13}C NMR spectra of regioregular polypropylene: (a) Zambelli, A.; Dorman, D. E.; Brewster, A. I. R.; Bovey, F. A. *Macromolecules* **1973**, *6*, 925. (b) Zambelli, A.; Locatelli, P.; Bajo, G.; Bovey, F. A. *Macromolecules* **1975**, *8*, 687. (c) Provasoli, A.; Ferro, D. R. *Macromolecules* **1977**, *10*, 874. (d) Tonelli, A. E. *Macromolecules* **1978**, *11*, 565. (e) Ferro, D. R.; Zambelli, A.; Provasoli, A.; Locatelli, P.; Rigamonti, E. *Macromolecules* **1980**, *13*, 179. (f) Zambelli, A.; Locatelli, P.; Provasoli, A.; Ferro, D. R. *Macromolecules* **1980**, *13*, 267. (g) Schilling, F. C.; Tonelli, A. E. *Macromolecules* **1980**, *13*, 270. (h) Zhu, S.-N.; Yang, X.-Z.; Chujo, R. *Polym. J.* **1983**, *15*, 859. (i) Asakura, T.; Omaki, K.; Zhu, S.-N.; Chujo, R. *Polym. J.* **1984**, *16*, 717. (j) Cheng, H. N.; Lee, G. H. *Macromolecules* **1987**, *20*, 436. (k) Hayashi, T.; Inoue, Y.; Chujo, R.; Asakura, T. *Polymer* **1988**, *29*, 138. (l) Miyatake, T.; Kawai, Y.; Seki, Y.; Kakugo, M.; Hikichi, K. *Polym. J.* **1989**, *21*, 809.

(3) Statistical analyses of ^{13}C NMR polypropylene configuration: (a) Doi, Y. *Makromol. Chem., Rapid Commun.* **1982**, *3*, 635. (b) Cheng, H. N. *J. Appl. Polym. Sci.* **1988**, *35*, 1639. (c) van der Burg, M. W.; Chadwick, J. C.; Sudmeijer, O.; Tulleken, H. J. A. F. *Makromol. Chem., Theory Simul.* **1993**, *2*, 399. (d) Busico, V.; Corradini, P.; De Biasio, R.; Landriani, L.; Segre, A. L. *Macromolecules* **1994**, *27*, 4521. (e) Busico, V.; Cipullo, R.; Corradini, P.; De Biasio, R. *Macromol. Chem. Phys.* **1995**, *196*, 491. (f) Busico, V.; Cipullo, R.; Corradini, P.; Landriani, L.; Vacatello, M.; Segre, A. L. *Macromolecules* **1995**, *28*, 1887.

(4) ^{13}C NMR investigations on regioirregular sequences and chain end-groups in polypropylene: (a) Zambelli, A.; Locatelli, P.; Bajo, G. *Macromolecules* **1979**, *12*, 154. (b) Zambelli, A.; Locatelli, P.; Rigamonti, E. *Macromolecules* **1979**, *12*, 156. (c) Asakura, T.; Nishiyama, Y.; Doi, Y. *Macromolecules* **1987**, *20*, 616. (d) Hayashi, T.; Inoue, Y.; Chujo, R.; Doi, Y. *Polymer* **1989**, *30*, 1715. (e) Cheng, H. N.; Ewen, J. A. *Makromol. Chem.* **1989**, *190*, 1931. (f) Zambelli, A.; Ammendola, P. *Prog. Polym. Sci.* **1991**, *16*, 203 and references therein. (g) Rieger, B.; Reinmuth, A.; Röll, W.; Brintzinger, H.H. *J. Mol. Catal.* **1993**, *82*, 67.

(5) (a) Shelden, R. A.; Fueno, T.; Tsunetsugu, T.; Furukawa, J. *J. Polym. Sci.: Part B* **1965**, *3*, 23. (b) Shelden, R.; Fueno, T.; Furukawa, J. *J. Polym. Sci.: Part A-2* **1969**, *7*, 763.

(6) Bovey, F. A.; Tiers, G. V. D. *J. Polym. Sci.* **1960**, *44*, 173.

(7) (a) Randall, J. C. *Polymer Sequence Determination—Carbon-13 NMR Method*; Academic Press: New York, 1977. (b) Bovey, F. A. *Chain Structure and Conformation of Macromolecules*; Academic Press: New York, 1982. (c) Tonelli, A. E. *NMR Spectroscopy and Polymer Microstructure: The Conformational Connection*; VCH Publishers: Deers Field, FL, 1989.

(8) In this paper, we define conventionally "routine" ^{13}C NMR spectra those recorded nowadays with spectrometers operating below 100 MHz. Of course, this definition does not apply to the pioneering studies cited on refs 2, 3, and 7, which were highly advanced when originally performed and still represent real milestones in the microstructural investigation of stereoregular vinyl polymers.

(9) (a) Barbè, P. C.; Cecchin, G.; Noristi, L. *Adv. Polym. Sci.* **1987**, *81*, 1. (b) Albizzati, E.; Giannini, U.; Morini, G.; Galimberti, M.; Barino, L.; Scordamaglia, R. *Macromol. Symp.* **1995**, *89*, 73.

(10) (a) Erker, G.; Nolte, R.; Tsay, Y. H.; Krüger, C. *Angew. Chem., Int. Ed. Engl.* **1989**, *28*, 628. (b) Erker, G.; Fritze, C. *Angew. Chem., Int. Ed. Engl.* **1992**, *31*, 199. (c) Erker, G.; Aulbach, M.; Knickmeier, M.; Wingbermühle, D.; Krüger, C.; Nolte, M.; Werner, S. *J. Am. Chem. Soc.* **1993**, *115*, 4590.

(11) (a) Mallin, D. T.; Rausch, M. D.; Lin, Y.-G.; Dong, S.; Chien, J. C. W. *J. Am. Chem. Soc.* **1990**, *112*, 2030. (b) Coates, G. W.; Waymouth, R. M. *Science* **1995**, *267*, 217. (c) Knickmeier, M.; Erker, G.; Fox, T. *J. Am. Chem. Soc.* **1996**, *118*, 9623.

(12) Ewen, J. A. *J. Am. Chem. Soc.* **1984**, *106*, 6355.

(13) (a) Kaminsky, W.; Külper, K.; Brintzinger, H. H.; Wild, F. R. W. P. *Angew. Chem., Int. Ed. Engl.* **1985**, *24*, 507. (b) Soga, K.; Shiono, T.; Takemura, S.; Kaminsky, W. *Makromol. Chem., Rapid Commun.* **1987**, *8*, 305. (c) Tsutsui, T.; Mizuno, A.; Kashiwa, N. *Makromol. Chem.* **1989**, *190*, 1177.

(14) (a) Busico, V.; Cipullo, R. *J. Am. Chem. Soc.* **1994**, *116*, 9329. (b) Busico, V.; Cipullo, R. *Macromol. Symp.* **1995**, *89*, 277. (c) Busico, V.; Cipullo, R. *J. Organomet. Chem.*, **1995**, *497*, 113. (d) Leclerc, M.; Brintzinger, H. H. *J. Am. Chem. Soc.* **1995**, *117*, 1651. (e) Resconi, L.; Fait, A.; Piemontesi, F.; Colonnesi, M.; Rychlicki, H.; Zeigler, R. *Macromolecules* **1995**, *28*, 6667. (f) Busico, V.; Caporaso, L.; Cipullo, R.; Landriani, L.; Angelini, G.; Margonelli, A.; Segre, A. L. *J. Am. Chem. Soc.* **1996**, *118*, 2105. (g) Leclerc, M.; Brintzinger, H. H. *J. Am. Chem. Soc.* **1996**, *118*, 9024.

(15) Ewen, J. A.; Razavi, A.; Elder, M. J. Eur. Patent Appl. 427696 (09.10.90).

(16) (a) Ewen, J. A.; Jones, R. L.; Razavi, A.; Ferrara, J. D. *J. Am. Chem. Soc.* **1988**, *110*, 6255. (b) Ewen, J. A.; Elder, M. J.; Jones, R. L.; Curtis, S.; Cheng, H. N. *Catalytic Olefin Polymerization*; Keii, T., Soga, K., Eds.; Kodansha: Tokyo, 1990; pp 439—482.

(17) (a) Farina, M.; Di Silvestro, G.; Sozzani, P. *Macromolecules* **1982**, *15*, 1451. (b) Farina, M.; Di Silvestro, G.; Sozzani, P.; Savarè, B. *Macromolecules* **1985**, *18*, 923. (c) Di Silvestro, G.; Sozzani, P.; Savarè, B.; Farina, M. *Macromolecules* **1985**, *18*, 928. (d) Farina, M.; Di Silvestro, G.; Sozzani, P. *Prog. Polym. Sci.* **1991**, *16*, 219.

(18) (a) Ewen, J. A.; Elder, M. J.; Jones, R. L.; Haspeslagh, L.; Atwood, J. L.; Bott, S. G.; Robinson, K. *Makromol. Chem., Macromol. Symp.* **1991**, *48/49*, 253. (b) Ewen, J. A.; Elder, M. J. *Makromol. Chem., Macromol. Symp.* **1993**, *66*, 179.
(19) Flory, P. J. *Statistical Mechanics of Chain Molecules*; Interscience Publishers: New York, 1969.
(20) Boyd, R. H.; Breitling, S. M. *Macromolecules* **1972**, *5*, 279.
(21) Suter, U. W.; Flory, P. J. *Macromolecules* **1975**, *8*, 765.
(22) Farina, M.; Di Silvestro, G.; Sozzani, P. *Macromolecules* **1993**, *26*, 946.
(23) Guerra, G.; Cavallo, L.; Moscardi, G.; Vacatello, M.; Corradini, P. *Macromolecules* **1996**, *29*, 4834.
(24) Of course, the different tacticity of the polymers must be taken into account. Just as an example, for a predominantly isotactic polypropylene sample, the main contribution to an $r(m)_{n-2}r$ *n*ad is given by the $rr(m)_{n-2}rr$ $(n + 2)$ad in the case of enantiomorphic-site control, by the $mr(m)_{n-2}rm$ $(n + 2)$ad in the case of chain-end control.
(25) This detection limit can be decreased significantly by increasing polymer concentration; however, this results in a lower resolution (see Experimental Section).
(26) (a) Grassi, A.; Zambelli, A.; Resconi, L.; Albizzati, E.; Mazzocchi, R. *Macromolecules* **1988**, *21*, 617. (b) Rieger, B.; Mu, X.; Mallin, D. T.; Rausch, M.; Chien, J. C. W. *Macromolecules* **1990**, *23*, 3559. (c) Busico, V.; Cipullo, R.; Chadwick, J. C.; Modder, J. F., Sudmeijer, O. *Macromolecules* **1994**, *27*, 7538.
(27) Stilbs, P.; Moseley, M. *Polymer* **1981**, *22*, 231.
(28) The question may arise whether classical 1D ^{13}C NMR is really the most suited technique for such detailed microstructural studies. On the point, we note that we do not know of any multidimensional sequence presently allowing to achieve a comparable digital resolution in F1. As a matter of fact, we have tested many proton-connected 2D sequences, both in direct and reverse mode, but the resolution of the ^{1}H spectrum was never good enough to ensure meaningful connectivities at the structural level of our interest. On the other hand, $^{13}C-^{13}C$ homocorrelated (INADEQUATE[33]) experiments cannot be used in this context due to their low sensitivity.
(29) Ernst, R. R.; Bodenhousen, G.; Wokaun, A. *Principles of Nuclear Magnetic Resonance in One and Two Dimensions*; Clarendon Press: Oxford, 1987; Chapter 4, pp 124−125.
(30) Shaka, A. J.; Barker, S. B.; Freeman, R. *J. Magn. Reson.* **1985**, *65*, 355.
(31) Segre, A. L.; Andruzzi, F.; Lupinacci, D.; Magagnini, P. L. *Macromolecules* **1983**, *16*, 1207.
(32) (a) Inoue, Y.; Nishioka, A.; Chujo, R. *Makromol. Chem.* **1973**, *168*, 163. (b) Randall, J. C. *J. Polym. Sci., Polym. Phys. Ed.* **1976**, *14*, 1693. (c) Schilling, F. C. *Macromolecules* **1978**, *11*, 1290.
(33) INADEQUATE is the acronym of "Incredible Natural Abundance Double Quantum Transfer Experiment"; see: Bax, A.; Freeman, R.; Kempsell, S. P. *J. Am. Chem. Soc.* **1980**, *102*, 4849.

MA970466A